

SUPPLEMENTARY MATERIAL FOR:

Synthetic biological circuits that demonstrate long-term genetic and functional stability in the mammalian gut

Authors:

David T Riglar^{1,2}, Tobias W Giessen^{1,2}, Michael Baym^{1,3}, S Jordan Kerns^{1,2} †, Matthew J Niederhuber^{1,2}, Roderick T Bronson⁴, Jonathan W Kotula^{1,2} ‡, Georg K Gerber⁵, Jeffrey C Way² & Pamela A Silver^{1,2*}.

Affiliations:

¹ Department of Systems Biology, Harvard Medical School, Boston Massachusetts, USA

²Wyss Institute for Biologically Inspired Engineering, Harvard University, Boston Massachusetts, USA

³ Department of Biomedical Informatics, Harvard Medical School, Boston, Massachusetts, USA

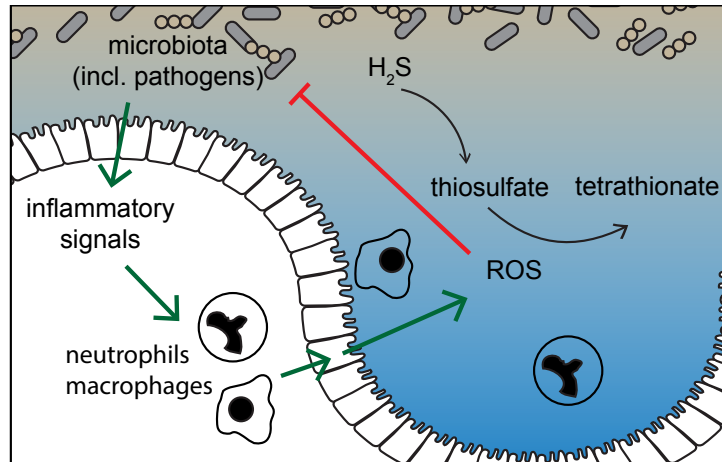
⁴ Department of Microbiology and Immunology, Harvard Medical School, Boston Massachusetts, USA

⁵ Massachusetts Host-Microbiome Center, Department of Pathology, Brigham and Women's Hospital, Harvard Medical School, Boston, Massachusetts, USA

† Current address: Emulate Inc., Boston, Massachusetts, USA

‡ Current address: SynLogic, Cambridge, Massachusetts, USA

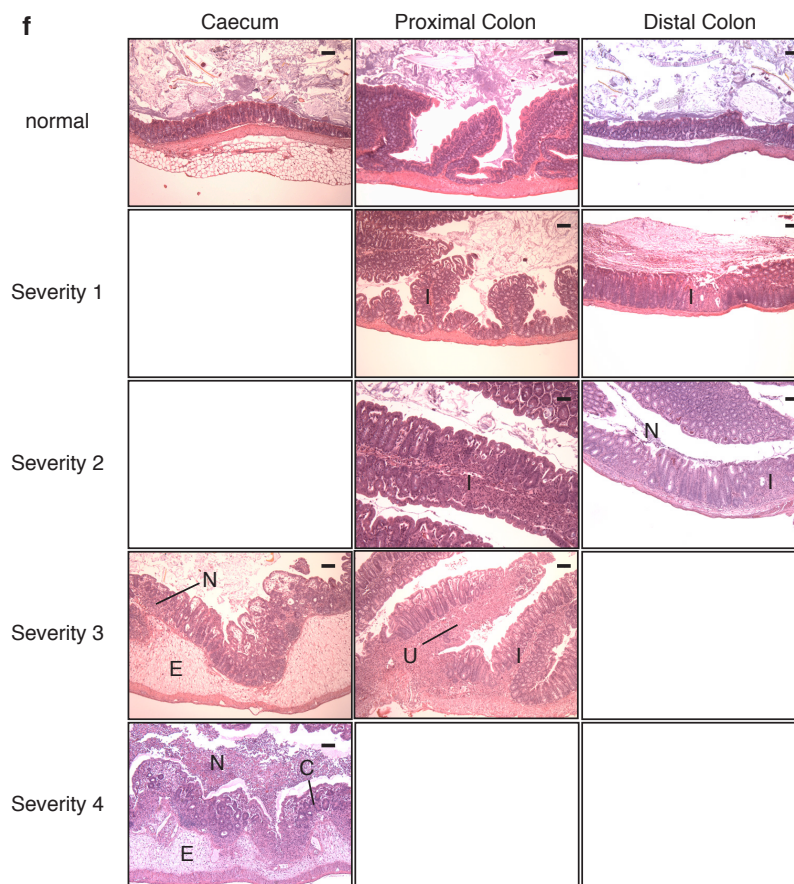
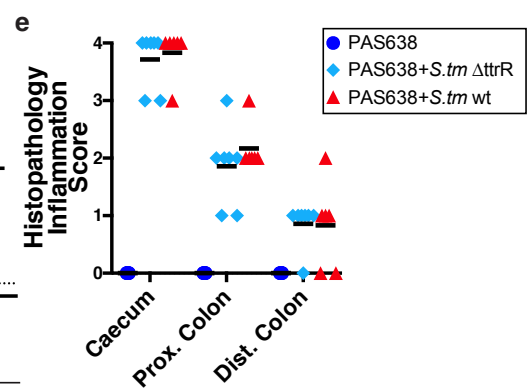
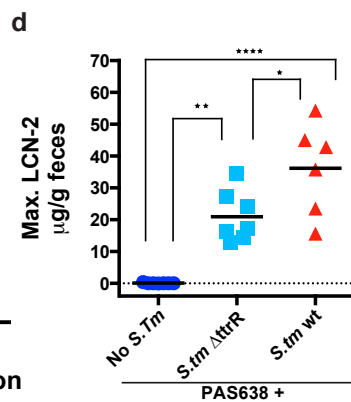
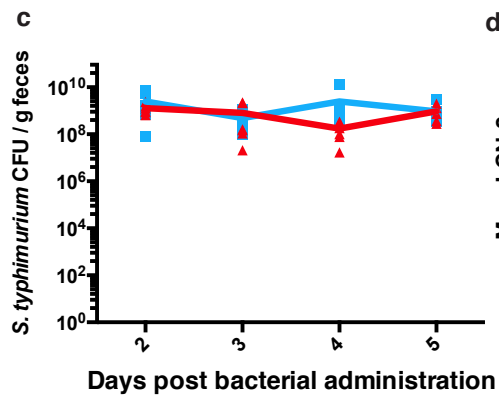
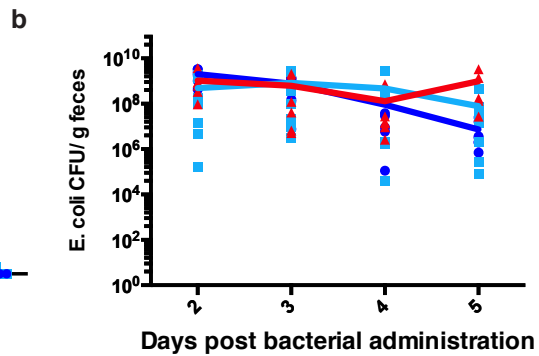
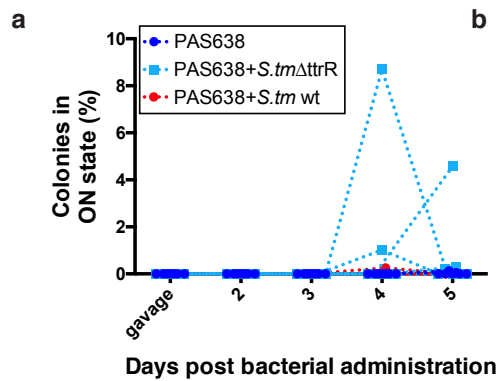
*Correspondence to: Pamela_Silver@hms.harvard.edu



Supplementary Figure 1

The inflammatory response in the mammalian gut leads to tetrathionate generation.

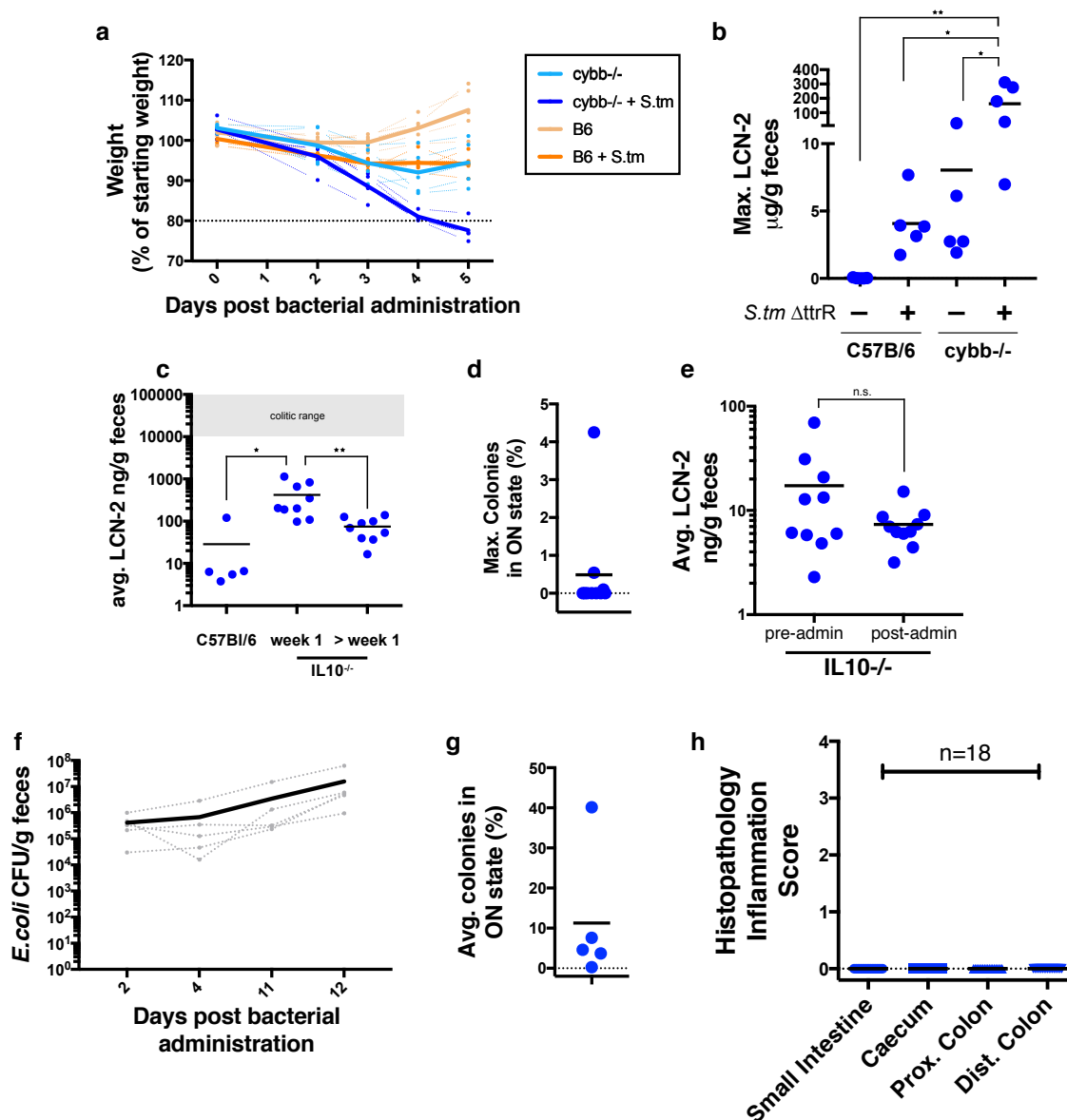
Cytokine signaling following an inflammatory insult leads to, among other responses, release of reactive oxygen species (ROS) into the gut lumen that inhibit microbial growth, and can oxidize thiosulfate, generated from hydrogen sulfide, to tetrathionate.



Supplementary Figure 2

PAS638 senses tetrathionate in a murine streptomycin-treated *S. typhimurium* colitis model

a) Timecourse of PAS638 switching during infection of C57Bl/6 mice with wt and $\Delta ttrR$ *S. typhimurium* (*S.ty*) (n= 6 for control and 7 for *S. typhimurium* infected groups). Switching was only apparent in colonies from mice co-infected with *S.typhimurium* $\Delta ttrR$ and on days 4 and/or 5 post administration. b) Enumeration of PAS638 *E. coli* and c) *S. typhimurium* variant levels by selective plating showed relatively consistent levels across experimental groups. d) LCN-2 quantification demonstrated inflammation in both *S. typhimurium* $\Delta ttrR$ and wt administered mice. Graphs show individual mouse values and mean. * p=0.02, ** p=0.001 *** p<0.0001, F(2,17) = 25.96, using one way ANOVA with Tukey's multiple comparisons test. e) Histology scoring of cecum, proximal and distal colon, showed inflammation in the presence of both *S. typhimurium* variants decreasingly apparent from the caecum to the distal colon. f) Scoring used a 0-4 point scale with example images of each score by histology provided. For cecal samples, only severity 3 and 4 were observed during *S. typhimurium* infection, characterized by accumulation of neutrophils (N) in epithelial tissues, edema (E), mucosal thickening and at times low-level presence of neutrophils in exudate at severity 3 and edema (E), extensive neutrophils present in exudate and/or epithelia (N), mucosal thickening and signs of crypt damage or regeneration (C) at severity 4. Proximal and distal colon showed signs of low-level inflammation (I) at severity 1, more extensive inflammation (I) and neutrophils in exudate (N) at severity 2. Severity 3 was noted in the proximal colon only and showed signs of ulceration (U), inflammatory cell migration (I), and neutrophils commonly present in exudate. Scale bars = 10 μ m.

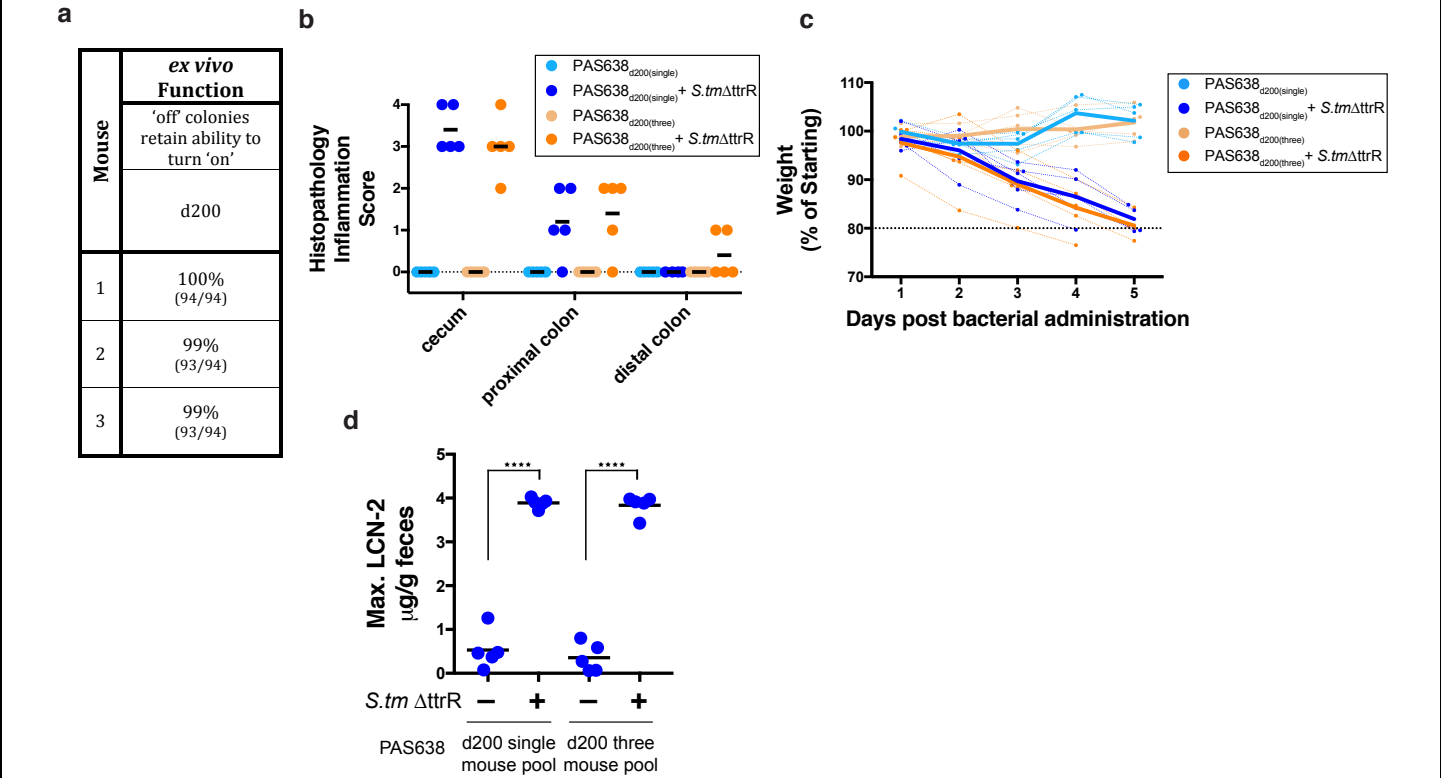


Supplementary Figure 3

PAS638 senses tetrathionate in *cybb*^{-/-}, *IL10*^{-/-}, and 129X1/SvJ mouse models.

a) Weight of *cybb*^{-/-} and C57Bl/6 control mice was measured following administration of PAS638 ± *S. typhimurium* (*S.tm*) Δ ttrR. Graph shows percentage of pre-administration weight of individual mice (dotted) along with group averages (solid line). b) Elevated LCN-2 levels were apparent in *S. typhimurium* Δ ttrR infected mice and *cybb*^{-/-} uninfected controls. Graph shows maximum measurements from days 3-5 following bacterial administration. Means are marked. **p*=0.01, ***p*=0.009, *F*(3,16) = 6.575, using one-way ANOVA analysis with Tukey's multiple comparison correction. For all other comparisons *p*>0.99. c) LCN-2 levels were elevated in *IL10*^{-/-} compared to control mice in the week following PAS638 administration therefore PAS638 measurements were taken >1-week following administration. Values are averages of 2-3 measurements from individual mice, with mean shown. **p*=0.02, ***p*=0.01, *F*(2,20) = 6.48 using one-way ANOVA test with Tukey's multiple comparison correction. >week 1 *IL10*^{-/-} samples were not significantly increased over C57Bl/6 controls (*p*=0.9). d) A subset of *IL10*^{-/-} mice administered PAS638 without streptomycin pre-treatment (*n*=10) showed elevated PAS638 switching. Graph shows maximum switching percentage from 4 measurements in the 12 days following administration. Mean is marked. e) When administered without streptomycin pre-treatment no indication of elevated LCN-2 levels was seen following

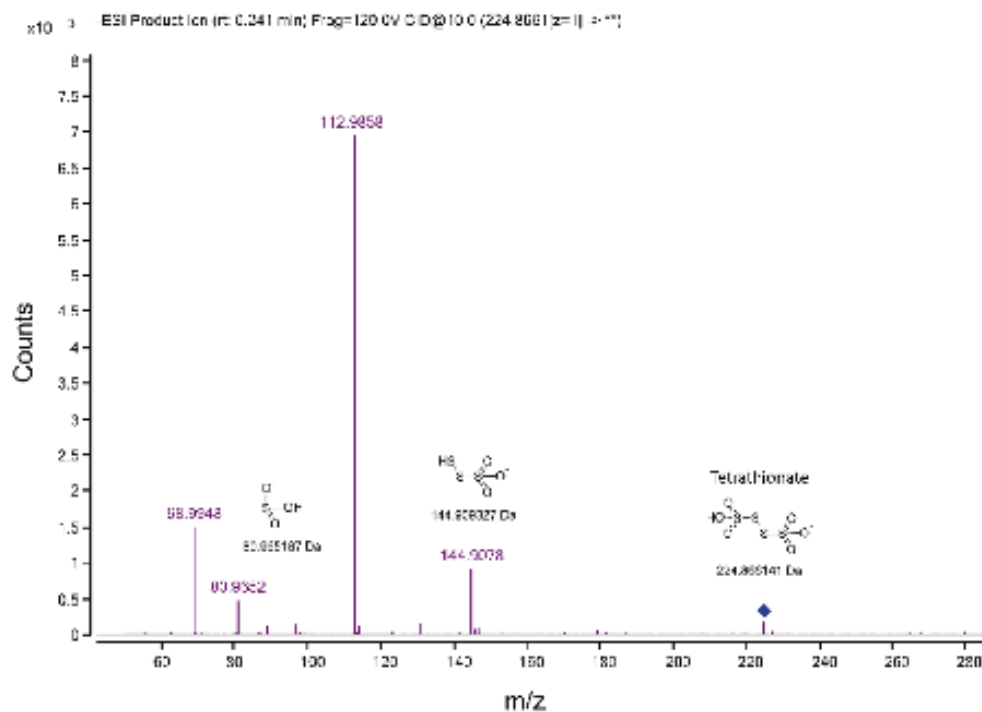
bacterial administration. Graph shows pre-administration levels (1 measurement) and average levels from 4 measurements in the 12 days following administration. Means are marked. n.s. = non-significant ($p = 0.6$) using a two-tailed Mann-Whitney test. f). PAS638 administered to 129X1/SvJ mice ($n=5$) without streptomycin pre-treatment colonized the gut successfully. Graph shows CFU values from individual mice (dotted lines) and average across the group (solid line). g) The absence of streptomycin pre-treatment did not affect PAS638 switching in these mice. Graph shows average switching from 4 measurements in the 12 days following bacterial administration. h) Histology scoring of small intestine, cecum, proximal and distal colon showed no signs of overt inflammation in 18 129X1/SvJ mice, including all that showed considerable switching by PAS638.



Supplementary Figure 4

Long-term stability of PAS638 during colonization of the mouse gut.

a) Essentially all PAS638 colonies tested following 200 days colonization in the 129X1/SvJ mouse (corresponding to Fig3e-f) retained *ex vivo* function when grown in the presence of sodium tetrathionate under anaerobic conditions. PAS638 colonies isolated after 200 days colonization were administered to C57Bl/6 mice \pm *S. typhimurium* (*S.tm*) Δ ttrR. b) Histology scoring of cecum and colon using a 0-4 point scale documented in Supplementary Fig. 2f detected elevated signs of inflammation in *S. typhimurium* Δ ttrR co-infected mice. c) *S. typhimurium* Δ ttrR infected mice also lost weight following infection (graph shows single mouse values (dotted lines) as percentage of pre-administration weight along with group averages (solid lines)) and d) showed elevated LCN-2 values. Graph shows maximum values measured from d1-5 post bacterial administration. ****p<0.0001 using separate two-tailed T-tests for the two individual experiments (t(8) = 16.55 and t(8) = 19.38 respectively). Means are shown.



Supplementary Figure 5

MS/MS fragmentation spectrum of tetrathionate

Exemplary fragmentation spectrum (MS/MS) of tetrathionate ($\text{M} = \text{S}_4\text{O}_6\text{H}_2$) detected in a cecum sample (see Fig. 2c). Negative ion mode and collision induced dissociation (CID) with nitrogen gas at 10 eV was used. The parent ion was isolated as $[\text{M}-\text{H}]$ at $m/z = 224.8661$. The corresponding chemical structures for the resulting fragments ($[\text{S}_3\text{O}_3\text{H}]^-$ and $[\text{SO}_3\text{H}]^-$) are shown in the spectrum.

Supplementary Table 1:**Strains constructed for use in this study.**

Strain name	Background	Elements (template)
PAS637	<i>E. coli</i> NGF1	LAM14 memory element and <i>rpsL</i> lys42arg Strep ^R (<i>E. coli</i> PAS132/133) ¹²
PAS638	<i>E. coli</i> NGF1	LAM14 memory element and <i>rpsL</i> lys42arg Strep ^R (<i>E. coli</i> PAS132/133) ¹² ; <i>ttrR/S-P_{ttrBCA}</i> (<i>S. typhimurium</i> LT2)
<i>S. typhimurium</i> wt (PAS639)	<i>S. typhimurium</i> 14028s	zhj-1401::Tn10 (<i>S. typhimurium</i> LT2 SA2700) (Salmonella Genetic Stock Database)
<i>S. typhimurium</i> Δ <i>ttrR</i> (PAS640)	<i>S. typhimurium</i> 14028s	zhj-1401::Tn10 (<i>S. typhimurium</i> LT2 SA2700) (Salmonella Genetic Stock Database); Δ <i>ttrR</i> (<i>S. typhimurium</i> LT2 TT22470) ¹⁸

Supplementary Table 2: GnotoComplex 2.0 strains. The strains chosen are human commensals selected to recapitulate key physiologic functions and phylogenetic diversity in the host.

Strain	ID
<i>Akkermansia muciniphila</i>	DSM 22959
<i>Anaerostipes hadrus</i>	DSM 3319
<i>Bacteroides cellulosilyticus</i>	DSM 14838
<i>Bacteroides fragilis</i>	ATCC 25285
<i>Bacteroides ovatus</i>	ATCC 8483
<i>Bacteroides vulgatus</i>	ATCC 8483
<i>Bifidobacterium longum subsp. infantis</i>	ATCC 15697
<i>Bilophila wadsworthia</i>	ATCC 51581
<i>Blautia hansenii</i>	DSM 20583
<i>Clostridium hiranonis</i>	DSM 13275
<i>Clostridium ramosum</i>	DSM 1402
<i>Clostridium scindens</i>	ATCC 35704
<i>Coprococcus comes</i>	ATCC 27758
<i>Dorea formicigenerans</i>	ATCC 27755
<i>Eggerthella lenta</i>	DSM 2243
<i>Enterococcus faecalis</i>	ATCC 29200
<i>Escherichia coli</i>	MG1655
<i>Klebsiella oxytoca</i>	ATCC 700324
<i>Lactobacillus reuteri</i>	DSM 20016
<i>Parabacteroides distasonis</i>	ATCC 8503
<i>Prevotella melaninogenica</i>	ATCC 25845
<i>Proteus mirabilis</i>	ATCC 29906
<i>Roseburia hominis</i>	DSM 16839
<i>Ruminococcus obeum</i>	ATCC 29174
<i>Veillonella parvula</i>	ATCC 10790